A Linear Switched Reluctance Motor Based Position Tracking System

S. W. Zhao*, N. C. Cheung*, Y. Lu *, W. C. Gan † and Z. G. Sun *

* Department of Electrical Engineering, Hong Kong Polytechnic University, Hong Kong, e-mail: *eencheun@polyu.edu.hk*

† Motion Group, ASM Assembly Automation Hong Kong Ltd., Hong Kong, e-mail: *wcgan@asmpt.com*

***Abstract*—A Linear Switched Reluctance Motor (LSRM) based position tracking system and its control aspect are presented in this paper. Based on modeling analysis of the drive system, two reduced order controlled models are developed with different time scales, referred as mechanical subsystem and electrical subsystem. Two controllers are respectively designed for the two subsystems. Simulation results demonstrate the effectiveness of this control scheme.**

***Keywords*—LSRM, position tracking system, winding excitation scheme.**

I. INTRODUCTION

Position tracking system is an essential element in advanced manufacturing processes. For demanding direct-drive applications, Linear Switched Reluctance Motors (LSRMs) have drawn much research attention over the past decade, due to its low cost, simple structure, ruggedness and reliability in harsh environments, and its potential for numerous industrial applications. Compared to rotary motors with mechanical transformation components for producing linear motion, LSRM has many advantages, such as quick response, high sensitivity and excellent tracking capability. Moreover, the structure of a LSRM can reduce the installation space requirement. However, the main limitation of the LSRM comes from its inherent nonlinear characteristics and force ripples problems which bring difficulties to its control.

Several control methods and schemes have been proposed in its control aspect. The most common method is to use a lookup table for the nonlinear torque/force compensation [1, 2]. Other literatures proposed nonlinear control methods for Switched Reluctance Motors (SRMs). A feedback linearization controller is designed for position tracking in [3], where two full-order nonlinear models are applied. In [4], an adaptive controller is presented to combat the nonlinear characteristics by the online estimation. In [5, 6], two passivity-based controllers are employed for SRMs and variable reluctance finger gripper, respectively. These control approaches provide possibilities to apply LSRM for building up a position tracking system. However, these control methods also require complicated control algorithms.

This paper is to propose a relatively simple control design which can be conveniently realized on a low cost embedded system for trajectory control applications.

II. SYSTEM CONSTRUCTION AND LSRM MODELING

A. Configuration of the drive system

The proposed drive system is shown in figure 1 (a). It can be seen that the mover is mounted on two linear guides, which are tightly fixed on the base. There are some ball bearings between the mover and these two linear guides. This rugged mechanical structure can effectively buffer vibration during the operations. A resolution linear optical encoder is integrated in the drive system to provide the feedback position information. The actuator of the drive system is a three-phase LSRM and its design schematic is shown in figure 1 (b). A set of three-phase coils with the same dimensions is installed on the mover.

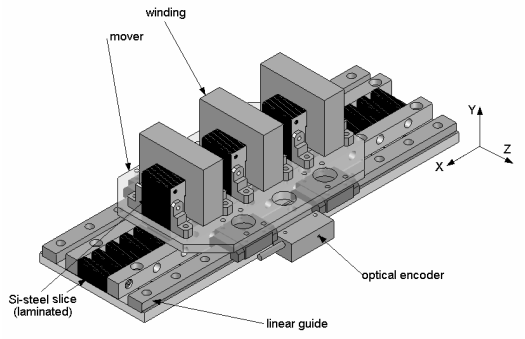

(a)

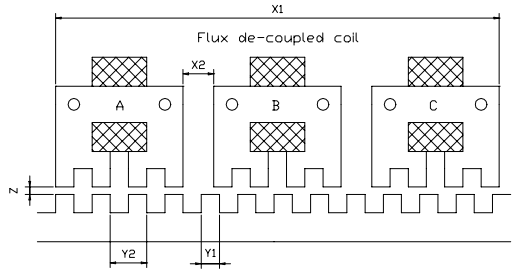

(b)

Fig. 1 Schematic of the drive system.

The body of the mover is manufactured with aluminum, so that the inertia of the mover is low and the magnetic circuits are decoupled. The stator track and the core of the

978-1-4244-1742-1/08/$25.00 ©

windings are laminated with silicon-steel plates, by means of which the motor manufacture can be simplified and the cost is reduced.

B. Modeling of LSRM

The dynamics of the whole drive system can be described as a combination of electromagnetic behaviors by a voltage equation as (1) and the mechanical movement as (2). The voltage equation can be further expressed as (3) since the flux linkage is a function of current and position.

$$V_j = r_j i_j + \frac{d\lambda_j}{dt}, j = a,b,c. \quad (1)$$

$$M\frac{dv}{dt} = \sum f_j - Bv - f_l. \quad (2)$$

$$V_j = r_j i_j + \frac{\partial \lambda_j}{\partial i_j}\frac{di_j}{dt} + \frac{\partial \lambda_j}{\partial x}v, j = a,b,c. \quad (3)$$

V_j denotes phase voltage, i_j denotes phase current, r_j denotes the winding resistance and λ_j denotes the phase flux linkage. x denotes the position and its derivate is the velocity v. The generated electromagnetic force is the sum of each phase force f_j, f_l denotes the external load force, M and B are the mass and friction constant. In linear case, phase force produced can be expressed as (4). L_j denotes phase inductance.

$$f_j(x,i_j) = \frac{1}{2}\frac{dL_j}{dx}i_j^2, j = a,b,c. \quad (4)$$

The response times of the electromagnetic behavior and mechanical motion are quite different. This is justified for our test setup since we can achieve the current loop bandwidth up to kHz while the output mechanical bandwidth is in the order of ten Hz [2]. Depended on the fact, the two-time-scale analysis is applied to model and design the drive system. The whole drive system is divided into two subsystems with different time scales named as fast and slow subsystem. In accord with the test results, the fast subsystem describes the electromagnetic behaviors of the coils while the slow subsystem corresponds to its mechanical motion.

III. Commutation and Winding Excitation Scheme of LSRM

As in SRMs, commutation is an important task for effectively operating LSRMs. This is derived from the fact that the direction of each phase force generated in a LSRM is dependent on its position. The desired force performance needs to be carried out by synchronous commutation with its position. However, the commutation results in the force ripples. To obtain a smooth output force, a force sharing strategy can be applied.

For any given position, there are two sets corresponding to the phases for positive force produced and the phases for negative force produced as follows,

$$\Theta^+ = \{j : \frac{\partial L_j(x)}{\partial x} \geq 0\} \text{ and } \Theta^- = \{j : \frac{\partial L_j(x)}{\partial x} < 0\}.$$

A force sharing strategy can be performed by a Force Distribution Function (FDF)

$$FDF(x, f_d) = f_d \begin{bmatrix} w_a(x) & w_b(x) & w_c(x) \end{bmatrix} \quad (5)$$

where f_d denotes the desired total force and w_j denotes the weight of force for phase j. A FDF should satisfy the principles as follows

$$\begin{cases} f_d \geq 0, w_j(x) > 0 \ \forall j \in \Theta^+ \text{ and } w_j(x) = 0 \ \forall j \in \Theta^- \\ f_d < 0, w_j(x) > 0 \ \forall j \in \Theta^- \text{ and } w_j(x) = 0 \ \forall j \in \Theta^+ \end{cases}. \quad (6)$$

$$\sum_{j=a}^{c} w_j(x) = 1. \quad (7)$$

The selection of weight depends on the various force sharing strategies on their design considerations. A phase inductance ratio based FDF is proposed for the phase current transition during its commutation in [8]. A simpler FDF scheme is proposed by using a linear switching in [2]. However, all of force sharing strategies should satisfy that the sum of each weight should be 1, which means that the sum of each phase force agrees with the desired total force.

As the linkage between the electrical subsystem and mechanical subsystem, a FDF and a current calculating function together are referred as the winding excitation scheme. The structure diagram of the winding excitation scheme is shown in figure 2. The FDF is used to calculate the desired phase force according to the position and the total desired force. The current calculate function is applied to calculate the desired phase current by using the desired phase force and the position.

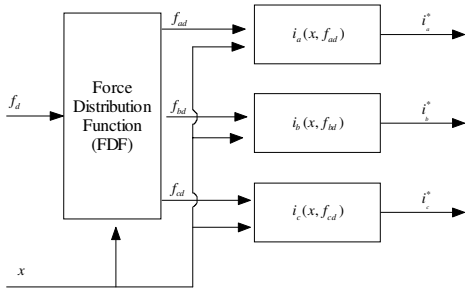

Fig. 2 The structure diagram of a winding excitation scheme.

According to force produced equation, the desired phase currents can be calculated by the output of the applied FDF and current calculating function. The precise model for flux linkage is hard to be obtained due to its inherent complexity. To calculate desired phase currents, the nonlinear flux linkage characteristics are usually approximated by a ratio function of phase inductance to displacement. Some methods have been proposed for approximating this ratio function. They can be classified into two groups: through a lookup table and through an approximation function. Lookup table only needs memory to store the characteristics data from the actual measurements; but it lacks flexibility. The approximation function needs more mathematical processing but it is more flexible for practical applications.

IV. CONTROLLER DESIGN FOR LSRM

The driving system adopts a cascaded control structure and two controllers are designed for the electromagnetic subsystem and mechanical subsystem corresponded to current control and position control, respectively. In the middle of the two control subsystems there is the applied winding excitation scheme. The block diagram of the whole driving system is shown as figure 3. In the cascaded control system, the inner loop is for current control with fast variables and the outer loop is for the position control with slow variables.

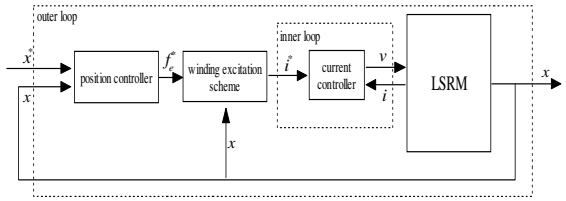

Fig. 3 Structure diagram of control scheme for position control.

For each phase coil, the relationship from terminal voltage to phase current can be approximated as a first-order differential equation. As the inner loop, it can be easily regulated by a proportional controller to guarantee both stability and quick response.

For the outer loop, the position controller can be designed from the energy dissipation viewpoint [7]. The state vector is defined as $X^T = \begin{bmatrix} x & v \end{bmatrix}$. The reduced-order model can be arranged as follows

$$D\dot{X} = [J - R]X + u + \xi \tag{8}$$

where $J = \begin{bmatrix} 0 & 1 \\ -1 & 0 \end{bmatrix}$, $R = \begin{bmatrix} 0 & 0 \\ 0 & B \end{bmatrix}$, $D = \begin{bmatrix} 1 & 0 \\ 0 & M \end{bmatrix}$, $u = \begin{bmatrix} 0 \\ \sum f_j \end{bmatrix}$ and $\xi = \begin{bmatrix} 0 \\ x - f_l \end{bmatrix}$.

The matrix J is a skew-symmetric, satisfied $J^T = -J$. The matrix R is a semi-positive definite symmetric matrix and corresponds to the energy dissipating of the model. D is a positive definite matrix. u denotes control vector and ξ denotes disturbance.

Define the state error as $E = X - X_d$ where X_d is the reference state vector. Substituting the state error into equation (8) yields the error model as

$$D\dot{E} + [R - J]E = \Phi \tag{9}$$

where $\Phi = -D\dot{X}_d - [R - J]X_d + u + \xi$.

The energy function of state error is chosen as

$$H(E) = \frac{1}{2} E^T D E . \tag{10}$$

It is clear that the error energy function is a non-negative function and its minimum is zero. By keeping the derivative of the energy function as zero on its equilibrium and negative in other region, the error energy function would be asymptotically dissipated to its minimum and the state variables would reach their desired. The derivative of the error energy function along time can be expressed as

$$\dot{H}(E) = E^T D\dot{E} . \tag{11}$$

The derivative can be rewritten as equation (12) by substituting equation (9) into equation (11). Equation (12) can be reformatted as equation (13) in that J is a skew-symmetric matrix and $E^T J E = 0$.

$$\dot{H}(E) = -E^T [R - J]E + E^T \Phi . \tag{12}$$

$$\dot{H}(E) = -E^T R E + E^T \Phi . \tag{13}$$

The asymptotical dissipation of the error energy function can be achieved by using the control signals from $\Phi = -KE$ where $K = diag\{k_1, k_2\}$, referred as damping injection matrix, is a positive define diagonal matrix. The derivative of error energy function can be further described as equation (14).

$$\dot{H}(E) = -E^T (R + K)E \tag{14}$$

In this case, $\dot{H}(0) = 0$ and $\dot{H}(E) < 0$ when $E \neq 0$ since $R + K$ is a positive definite diagonal matrix.

V. SIMULATION RESULTS

In this section, the performance of the proposed algorithm is illustrated by simulations, which are achieved by the MATLAB software package. Figure 4 shows the position tracking results and force signals of square waveform. It is clear that the system accurately tracks the reference and actual force matches force reference well.

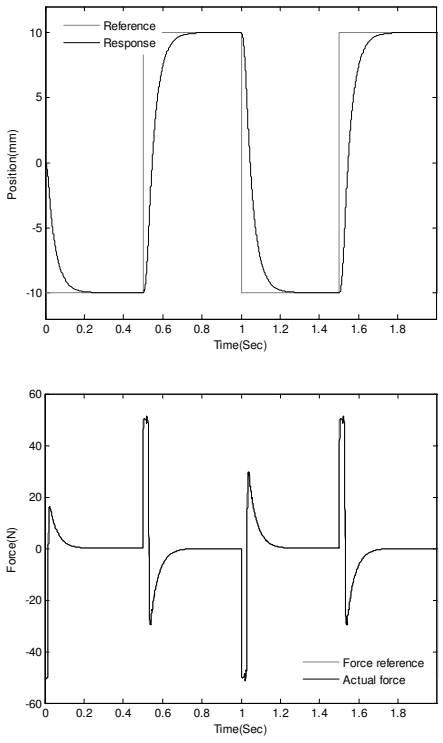

Fig. 4 Simulation: position tracking and its control signal waveforms.

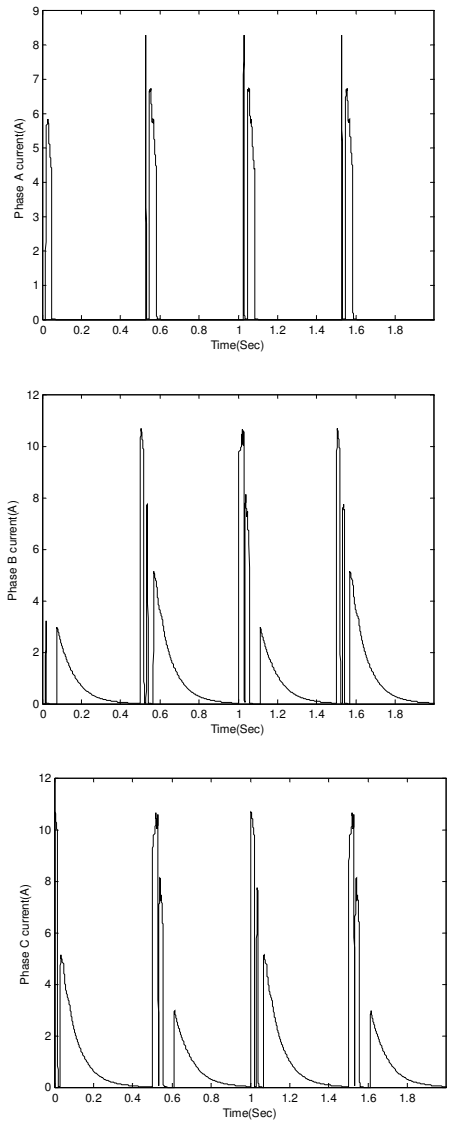

Fig. 5 Simulation: phase current waveforms.

The corresponded phase currents are shown in figure 5. Notice that all the phase currents are switched on and switched off continuously to perform the desired force.

VI. CONCLUSIONS

In this paper, a simple yet effective control design is represented for a LSRM based position tracking system is proposed. The whole drive system is decomposed into two subsystems with different time scales. Following that, the position controller and current controller are designed for the two subsystems respectively. Simulations demonstrate the effectiveness of this control scheme.

ACKNOWLEDGMENT

The authors would like to thank the University Grants Council for the funding support of this research work through project codes: PolyU 5224/04E and PolyU 5141/05E.

REFERENCES

[1] D. G. Taylor, "An experimental study on composite control of switched reluctance motors," *IEEE Contr. Sys. Magazine*, Vol. 11, Issue 2, pp. 31-36, Feb. 1991.

[2] W. C. Gan, N. C. Cheung and L. Qiu, "Position control of linear switched reluctance motors for high precision applications," *IEEE Trans. Ind. Applicat.*, Vol. 39, Issue 5, pp.1350-1362, Step. /Oct. 2003.

[3] M. Ilic'-Spong, R. Marino, S. M. Peresada and D. G. Taylor, "Feedback linearizing control of switched reluctance motors," *IEEE Trans. Automat. Contr.*, Vol. AC-32, pp. 371-379, May 1987.

[4] S. A. Bortoff, R. R. Kohan and R. Milman, "Adaptive control of variable reluctance motors: a spline function approach," *IEEE Trans. Ind. Electron.*, Vol. 45, Issue 3, pp.433-444, Jun 1998.

[5] G. Espinosa-Pérez, P. Maya-Ortiz, M. Velasco-Villa and H. Sira-Ramíez, "Passivity-based control of switched reluctance motors with nonlinear magnetic circuits," *IEEE Trans. Contr. System Tech.*, Vol. 12, Issue 3, pp. 439-448, May 2004.

[6] K. K. Chan, J. M. Yang and N. C. Cheung, "Passivity-based control for flux regulation in a variable reluctance finger gripper," *IEE Pro.-Electr. Power Appl.*, Vol. 152, Issue 3, pp. 686-694, May 2005.

[7] R. Ortega, A. J. van ser Scharf, I. Mareels and B. Maschke, "Putting energy back in control," *IEEE Contr. Sys. Magazine*, Vol. 21, Issue 2, pp. 18-33, Apr. 2001.

[8] H. K. Bae, B. S. Lee, P. Vijayraghavan and R. Krishnan, "A linear switched reluctance motor: converter and control," *IEEE Trans. Ind. Applicat.*, vol 36, pp. 1351-1359, Sep. /Oct. 2000.